ACS OMEGA

Open Access

http://pubs.acs.org/journal/acsodf

Article

Simple and Rapid Method of Microwell Array Fabrication for Drug Testing on 3D Cancer Spheroids

Mai Anh Nguyen, Nhung Thi Dinh, My Hanh Do Thi, Dung Nguyen Thi, Uyen Thu Pham, Toan Quoc Tran, Vuong Minh Nguyen, Nhung Hong Le, Duong Thanh Nguyen,* and Dung Thuy Nguyen Pham*

Cite This: *ACS Omega* 2024, 9, 16949−16958

Read Online

ACCESS | Metrics & More | Article Recommendations

ABSTRACT: Three-dimensional (3D) cell culture systems are becoming increasingly popular due to their ability to mimic the complex process of angiogenesis in cancer, providing more accurate and physiologically relevant data than traditional two-dimensional (2D) cell culture systems. Microwell systems are particularly useful in this context as they provide a microenvironment that more closely resembles the in vivo environment than traditional microwells. Poly(ethylene glycol) (PEG) microwells are particularly advantageous due to their bio-inertness and the ability to tailor their material characteristics depending on the PEG molecular weight. Although there are several methods available for microwell fabrication, most of them are time-consuming and expensive. The current study utilizes a low-cost laser etching technique on poly(methyl methacrylate) materials followed by molding with PDMS to produce microwells. The optimal conditions for making concave microwells are an engraving parameter speed of 600 mm/s, power of 20%, and a design diameter of the microwell of 0.4 mm. The artificial tumor achieved its full size after 7 days of cell growth in a microwell system, and the cells developed drugs through a live/dead assay test. The results of the drug testing revealed that the IC_{50} value of zerumbone-loaded liposomes in HepG2 was 4.53 pM, which is greater than the IC_{50} value of zerumbone. The HepG2 cancer sphere's 3D platform for medication testing revealed that zerumbone-loaded liposomes were very effective at high doses. These findings generally imply that zerumbone-loaded liposomes have the capacity to target the liver and maintain medication delivery.

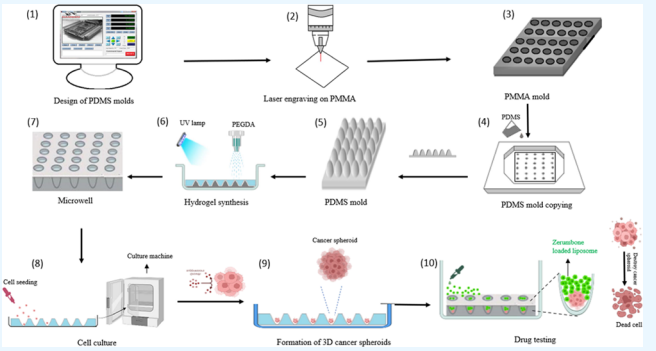

1. INTRODUCTION

Cancer is a major public health concern with an alarming prevalence and a leading mortality rate worldwide.[1] According to the International Agency for Research on Cancer, there were 19.3 million new cases of cancer and 10 million cancer-related deaths in 2020.[2] In addition, global demographic characteristics predict an increased cancer incidence in the next decades, with 420 million new cancer cases by 2025.[3] Therefore, effective treatment strategies are of paramount importance in reducing the burden of cancer on individuals and societies.

Contemporary cancer management modalities comprise an assortment of interventions, including chemotherapy, surgery, hormone therapy, radiation therapy, adjuvant therapy, and immunotherapy.[4] Of these, chemotherapy stands out as a prominent and efficacious treatment strategy for neoplastic ailments. However, the development of chemotherapy drugs entails an intricate and costly process that requires a substantial investment of time, resources, and expertise. Moreover, differences between in vitro and in vivo research undermine the accuracy and dependability of results from predicting drug toxicity and efficacy models in people, causing the high rejection rate of candidates with one out of 10,000 laboratory-created compounds being commercialized.[5−10] Therefore, a novel in vitro testing method to reduce and eliminate unsuitable chemicals and select more precise molecules for further tests is necessary for drug development.

Some methods for screening anticancer drugs in the field today include DNA synthesis cell proliferation assay, clonogenic cell survival assay, methods based on metabolic activity, etc. However, the above methods all have the same drawback: time; some methods require indirect measurement. In addition, DNA synthesis cell proliferation assay also requires

Received: August 9, 2023
Revised: November 30, 2023
Accepted: December 12, 2023
Published: April 5, 2024

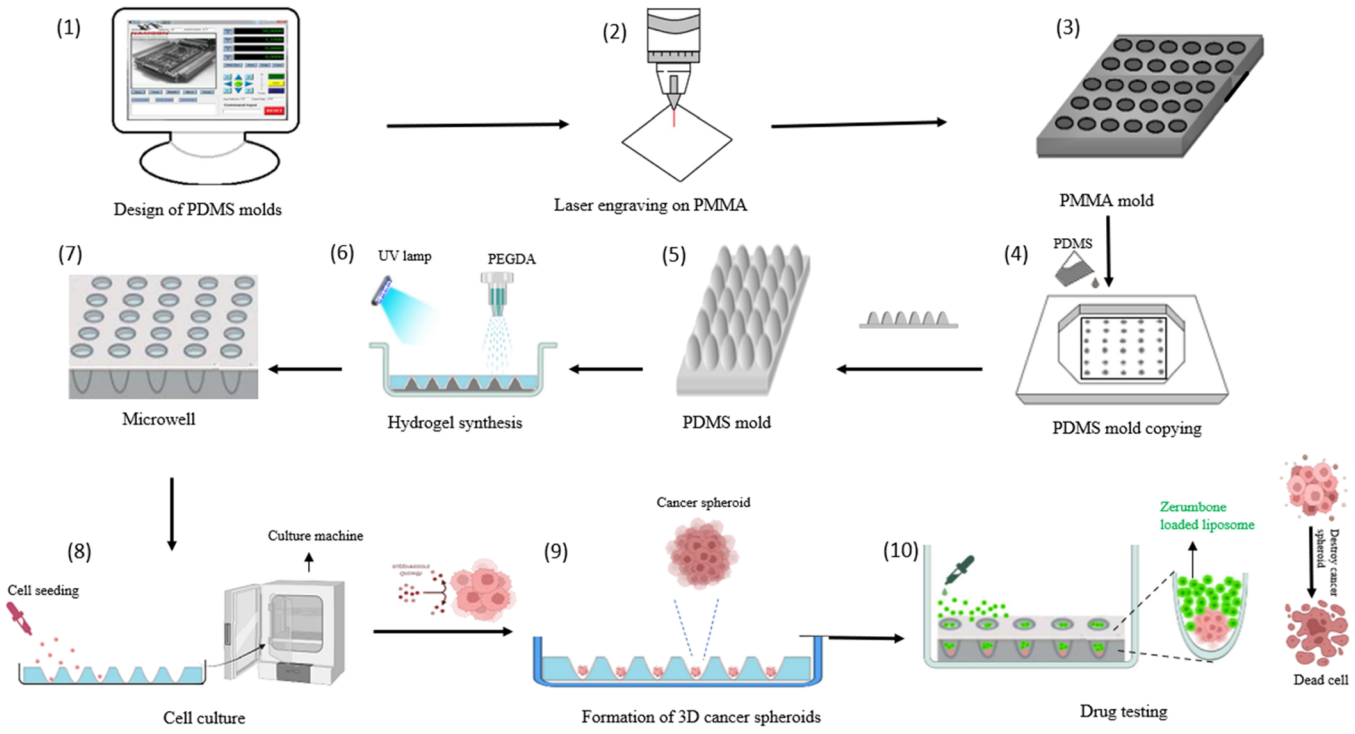

Figure 1. Schematic of microwell fabrication. The process involved (1) designing a PMMA mold using graphical software and (2) laser-cutting and etching PMMA sheets to create the desired shape; (3−5) resulting PMMA mold was then used to cast a polydimethylsiloxane (PDMS) mold, (6, 7) which was subsequently inserted into a hydrogel mixture to create microwells; (8) cancer cells were then seeded into the microwells and (9) cultured in an incubator to form spheroids; (10) these spheroids were utilized for drug testing.

the use of radioactive labels and is required to be performed only in vitro or ex vivo and cannot perform any further research with cells.[11] Liposome-assisted drug delivery is known to be an effective delivery system due to their physicochemical and physiological properties, which enable them to stabilize therapeutic compounds, overcome obstacles to cellular and tissue uptake, and improve the biodistribution of compounds to target sites in vivo.[12]

3D cell culture has been widely applied in various fields, including medicine, molecular biology, cell biology, and pharmacology. Cells on 3D culture platforms have attracted a lot of interest in drug testing models, and a variety of culture technologies has been developed.[13,14] Zhang et al. used a scaffold-based 3D culture system to test the effectiveness of a drug for treating breast cancer.[15] They found that the 3D culture system provided a more physiologically relevant environment than traditional 2D cell culture and that the drug was more effective in inhibiting cancer cell growth in the 3D system. However, scaffold-based 3D culture systems have certain limitations, including difficulty in controlling scaffold degradation, a lack of physiological complexity, and variability in cell behavior. Scaffold-based systems can also have limitations in terms of scalability and reproducibility, as well as potential interference with imaging and analysis techniques.[16] The hanging drop method used by Helena Topouzi and colleagues is a 3D cell culture technique that involves suspending cells in a droplet of medium that is inverted on a Petri dish lid.[17] However, this method has limitations in controlling the size of the cell aggregates and the accuracy of the measurement results.[18] Similarly, the method of using nonadherent surfaces to culture cancer cells and form 3D spheroids was performed by a research group led by Yip.[19] This method allows for the formation of spheroids with a more uniform size and shape compared to those of the hanging drop method. However, similar to the hanging drop method, this method also has limitations in controlling the size of spheroids and the accuracy of measurement results.[18]

On the other hand, microwell technology is another commonly used method to create 3D structures that mimic the in vivo tissue architecture.[18] It offers a controlled and defined environment for cells to grow and interact with each other. One of the advantages of using microwells for 3D cell culture is the precise control over the size and shape of the resulting structures.[20,21] This can enhance the reproducibility and reliability of experiments. Additionally, microwells can be utilized to develop high-throughput screening platforms for drug discovery and toxicity testing.[22,23] The small and compact wells allow for processing large numbers of samples in parallel, thus increasing the efficiency and throughput of experiments.

Microwells can be generated through various fabrication techniques, which include but are not limited to lithography, soft lithography, microcontact printing, and direct micromachining.[24−26] The lithography method has been used by many research groups to create microwells.[27,28] The advantage of this method is its high precision and reproducibility as well as the ability to create large arrays of microwells. However, the main limitation is that it requires expensive equipment and expertise in photolithography.[14] Besides, direct microwell fabrication is simple and low-cost and can create microwells of various shapes and sizes.[29,30] However, the main limitation is that it can be time-consuming and difficult to control the exact size and shape of the microwells. Soft lithography, which employs elastomeric stamps or molds, is another utilized manufacturing technology for microwell production.[21] However, the procurement of certain mold materials can pose a challenge due to their high cost and limited availability. Given

https://doi.org/10.1021/acsomega.3c05873
ACS Omega 2024, 9, 16949−16958

the advantages and limitations of the various microwell fabrication methods, there is a need for faster and more convenient solutions that can create microwells with high precision and reproducibility while also being low-cost and easy to use.

Laser engraving is the most recent method and has served as an enabling and reliable tool for rapid and cost-effective microwells over the past few decades.[31] The laser engraver setup is lead due to its low operational power, lightweight, handiness, and very easy-to-learn features. When using a laser for the process of engraving, there is no wear on the tool along with more accuracy obtained.[32] Laser CO_2 is one of the laser sources used for rapid prototyping and cost-effective microfabrication. Microchip etching is a rapid fabrication method for microfluidic devices.[33] Laser ablation is used to create microstructures on polymer materials. Adjusting the power, pulse, and focal plane position of the laser can help control the depth and shape of the microwells.[34] Microwells are considered qualified when suitable for cell growth and are cost-effective, have symmetry and volume sufficient to accommodate the required number of cells, and have low surface roughness to avoid damaging cells.[35] Looking from above, we see an elliptical concave well system with two protruding structures along the horizontal axis.[36]

Therefore, in this study, we present a novel technique for creating microwell molds. Figure 1 provides an overview of the manufacturing, testing, and assessment processes employed for the microwells investigated in this study. The microwells were designed and machined using laser engraving and subsequently replicated using polydimethylsiloxane (PDMS) and PEGDA. Subsequently, the microfluidic wells were seeded with cells, leading to spheroid formation and 14-day culture. The resulting spheroids were subjected to a live/death assay, followed by evaluation with zerumbone-loaded liposomes. This new approach will offer a useful and effective tool for drug testing and support the use of chemotherapy for more significant purposes in cancer treatment.

2. MATERIAL AND METHODS

2.1. Materials. The laser machine system was manufactured in China and was monitored by Phan Long Laser Company (Vietnam) with the requested laser parameter. Poly(methyl methacrylate) (PMMA) sheets with thicknesses of 3 and 5 mm were obtained from Fusheng (Taiwan). Phosphate buffered saline (PBS), poly(ethylene glycol) diacrylate (PEGDA), and photoinitiator (PI) were purchased from Sigma-Aldrich (St. Louis, MO, USA). Human liver cancer cell line (HepG2) was obtained from ATCC (Manassas, VA, USA). Fetal bovine serum (FBS) and penicillin-streptomycin (PS) were purchased from Sigma-Aldrich (St. Louis, MO, USA). Dulbecco's modified Eagle's medium (DMEM) microfluidic medium was acquired from Thermo Fisher Scientific (Waltham, Massachusetts, USA). Zerumbone was a gift from associate professor Luong Ngo from Hong Duc University by extraction from *Costus Speciosus Smith*. Dimethyl sulfoxide (DMSO), and Tween 20 were purchased from Sigma Chemical Co. (St. Louis, MO, USA). Live/Dead assay including Calcein AM, ethidium homodimer, was obtained from Introvigen (MA, USA). Red and blue dyes of food color liquids were obtained from Vinh Nam Anh Co., Ltd. (Vietnam)

2.2. Methods. *2.2.1. Synthesis of Microwell PMMA Molds.* The PMMA mold was previously designed in Adobe Illustrator and AutoCAD software and imported into the laser machine for the cutting and engraving. The microwells are created with different parameters using a laser beam to etch the surface of a 5 mm thick sheet of PMMA to form PMMA molds. To investigate the effects of laser speed to the structure of microwells, the laser intensity was fixed at 20% and the speed was adjusted from 500 to 1400 mm/s (step length was 100 mm/s). Similarly, the effects of laser power on microwell formation were investigated by keeping the laser speed constant at 600 mm/s and altering power values from 10 to 100% (step length was 10%). Furthermore, multiple diameters of etched patterns (ranging from 0.1 to 0.6 mm) at 20% power and a speed of 600 mm/s were studied at 20% power and a speed of 600 mm/s in order to determine the ideal diameter of microwells for spheroid cultivation. After completion, the PMMA molds were cleaned and examined under an electronic microscope; the depth and width of microwells were measured using ImageJ (National Institute of Health, USA).

2.2.2. Synthesis of PEG Microwells. The PDMS mold was fabricated by copying the PMMA microwell molds. PDMS was prepared by mixing the base elastomer with a curing agent in a 10:1 (v/v) ratio of the prepolymer. After degassing for half an hour, 10 mL of the PDMS mixture was poured into the cup containing the PMMA mold. PDMS stamp was removed from the mold after curing for 12 h at room temperature and cleaned with ethanol 70% before creating hydrogel microwells. Fifteen milliliters of the solution consisting of 89.9% PBS, 10% PEGDA, and 0.1% PI were used to fabricate microwells, 50 μL of the solution was dropped into the PDMS stamp, and PEG microwells were formed after irradiating the solution with UV light for 2 min to allow thermal polymerization to take place. The products were stored at room temperature in PBS solution, and the width and the depth were measured on days 1, 3, 5, and 7.

2.2.3. Formation of 3D Cancer Spheroids. The PEG microwell was cleaned with PBS twice before cell seeding. A cell solution with a concentration of 2×10^5 cells/mL was prepared and instilled into the microwells. The cells were allowed to settle in the cultured microwells for 5 min. Excess cells were then removed by washing the device with 3 mL of DMEM medium. To monitor cancer spheroid growth and viability, cells were cultivated in a DMEM medium including 10% FBS at 37 °C in a 5% CO_2 incubator for 10 days. The DMEM cultures were replenished after 24 h, and cancer spheroids were observed development at specific time points: on day 1, day 3, day 5, day 7, and day 10. The live/death assay was applied to provide evidence of the spheroids' viability in the microfluidic system in incubation.

2.2.4. Drug Testing. In the previous report, the process of synthesizing zerumbone-loaded liposomes involved the utilization of the film hydration method, which was followed by extrusion.[7] Liposomes were synthesized through a process involving thin film hydration followed by extrusion. Initial solutions of Cholesterol, DOPC, and zerumbone in $CHCl_3$ were prepared. These solutions were combined, vortexed, and transferred to a round-bottom flask for solvent removal. The resulting thin film was hydrated, sonicated, and dialyzed to obtain a liposome suspension. This suspension underwent extrusion and was stored at room temperature. Blank liposomes were also prepared without zerumbone. The liposomes' size, zeta potential, and polydispersity index were analyzed using a Zetasizer Nano ZS. Storage stability was evaluated by measuring liposome size and the amount of

https://doi.org/10.1021/acsomega.3c05873
ACS Omega 2024, 9, 16949−16958

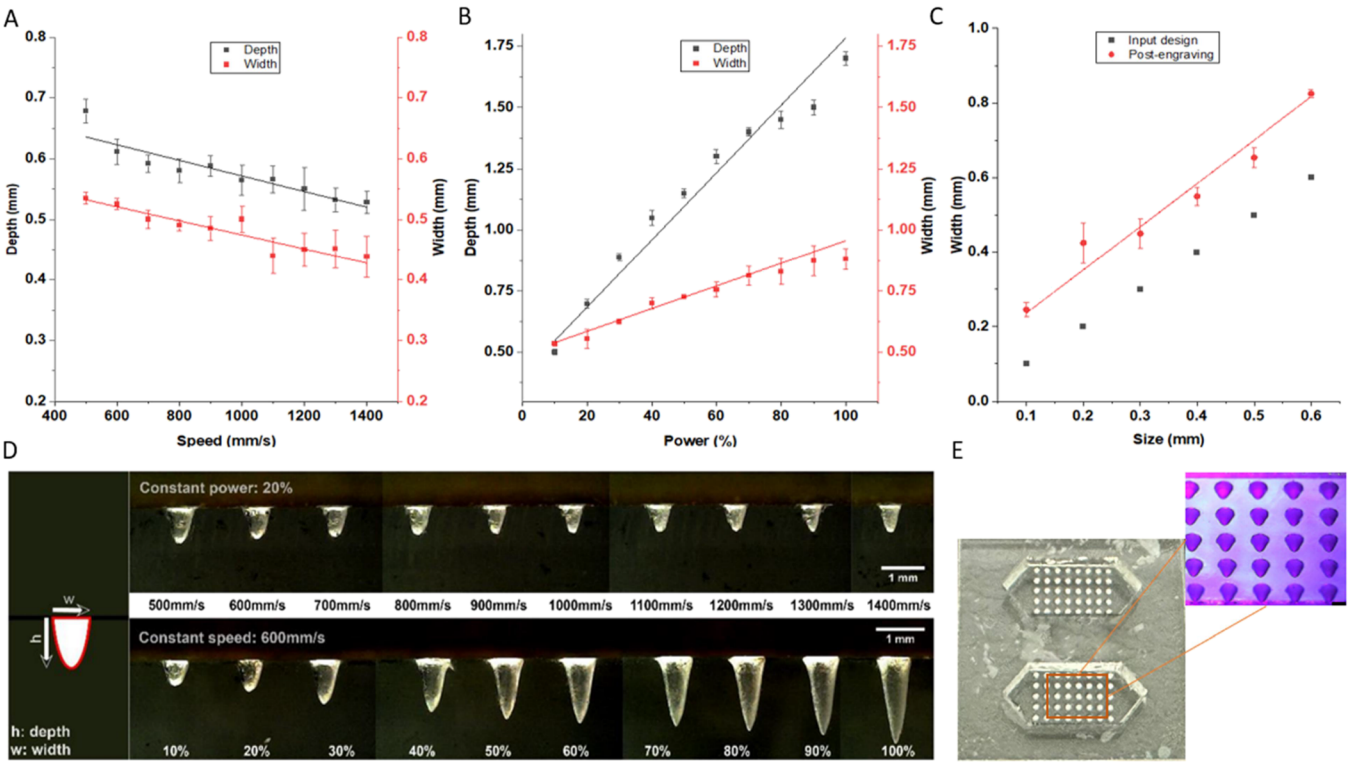

Figure 2. Influence of laser-engraving factors on the microwells was investigated. (A) Change in the width and depth of microwells with increasing laser speeds. (B) Effect of power on the width and depth of microwells. (C) Width difference between postengraving and input design. (D) Microwells with changing velocity and power (scale bar = 1 mm). (E) Series of microwells for cell culture (scale bar = 500 μm).

encapsulated zerumbone 7 days after synthesis.[7] Storage stability was evaluated by measuring liposome size and the amount of encapsulated zerumbone 7 days after synthesis 7. Blank liposome, zerumbone, and zerumbone-loaded liposome were mixed in DMEM medium supplemented with 10% FBS to obtain the desired concentrations (0.1, 1, 5, 10, 20 μM), and were introduced into the microwells. After culturing for 24 h for cultivation, cell viability was examined. The formula for drug loading content and encapsulation efficiency has been presented by us in previous research.[7]

2.2.5. Cell Viability. For cell cultivation, the process has been reported in our previous study.[14] Cell viability was evaluated using CaAM/EthD-1 staining. Each follicle was incubated independently for 30 min at 37 °C with 5 μmol/L ethidium homodimer and μmol/L Calcein AM in the dark. Living cells are nonfluorescent cells that have been invaded by Calcein-AM. Living cells emit green fluorescence, which was detected by the excitation/emission 495/635 nm wavelength. Dead cells result in a bright red fluorescence with approximately 495/635 nm of excitation/emission from bonding with ethidium homodimer-I, which enters the cells through the broken membranes and attaches to nucleic acids.[37] After washing twice with medium, samples were examined with an Olympus Fluorescence Microscope. The image of cell viability was taken and using the ImageJ software (Bethesda, Maryland, USA) to analyze the viability.

2.2.6. Statistical Analysis. Three biological replicates of the trial were used to determine the mean and standard deviation, which are shown as error bars. Student *t*-tests were employed in all experiments for statistical analysis, and the data were presented by OriginPro 2022 and GraphPad Prism 9.

3. RESULTS AND DISCUSSION

3.1. Characterization of Laser Engraving Parameters.

Figure 2 shows the influence of the laser-engraving factors on microwells. In order to investigate the relationship between laser speed and geometry of microwells, the laser power was fixed at 20%, while laser speed was 500, 600, 700, 800, 900, 1000, 1100, 1200, 1300, and 1400 mm/s. The increase in laser speed observed the decline of both the depths and widths of microwells as shown in Figure 2A. The microwells' depth considerably lowered from 0.68 to 0.58 mm, increasing in tandem with the laser's speed from 500 to 800 mm/s. However, the depth of microwells rose to 0.6 mm at 900 mm/s laser speed but decreased from 0.57 to 0.52 mm when the laser speed was raised from 1000 to 1400 mm/s. Similarly, the width of microwells also reduced from 0.52 to 0.48 mm, when the laser speed increased 500−900 mm/s. The width of microwells significantly increased to 0.5 mm at the 1000 mm/s laser speed, then significantly shrunk to approximately 0.44 mm when the laser speed rose from 1100 to 1400 mm/s.

The exact shapes of the microwells and the relationship between laser speed and the depth of microwells are illustrated in Figure 2B. At higher engraving speeds, the engraving depth reduces as the laser beam spends less time at each point, resulting in less heat absorption by the material and a shallower and narrower microchannel.[36−38]

In order to investigate the relationship between laser power and the geometry of microwells, the laser speed was fixed at 600 mm/s, and the laser power levels were set to 10, 20, 30, 40, 50, 60, 70, 80, 90, and 100%. Figure 2A depicts the increase of the laser power, increasing the depth and width of the microwells. When the laser power increased from 10 to 60%, the depth of microwells grew dramatically from 0.5 to 1.35

https://doi.org/10.1021/acsomega.3c05873
ACS Omega 2024, 9, 16949−16958

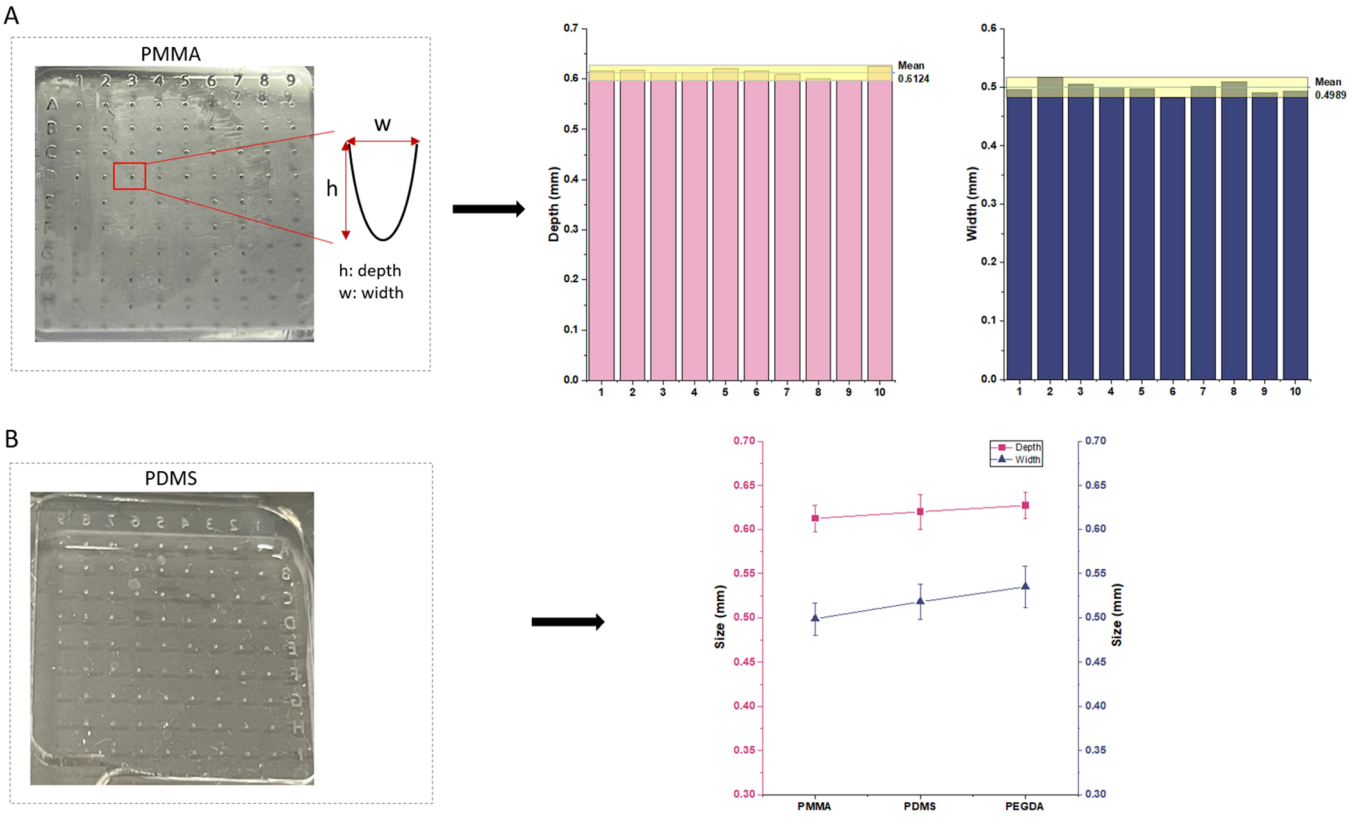

Figure 3. Comparison of the microwell size in PMMA, PDMS, and PEGDA. (A) Depth and width uniformity of 10 microwells in PMMA molds after laser engraving. (B) Comparison in depth and width of PMMA mold, PDMS copying, and PEGDA copying.

mm. When the laser power was raised to 80%, the depth of the microwells grew significantly to 1.5 mm, and at 100% laser power, the depth of the microwell was 1.73 mm. The width of microwells also increased when the laser power increased, although at a slower rate than the depth of the When the laser power was raised from 10 to 40%, the width of the microwells rose dramatically from 0.51 to 0.75 mm, and when the laser power was increased from 50 to 100%, the width grew from 0.74 to 0.88 mm.

Figure 2B illustrates that as the laser power was increased from 40 to 100%, the tip of the microwells became sharper. This results can be explained based on the increased power, which can be associated with a greater amount of energy transferred to the PMMA surface, leading to the removal of larger material volumes and the generation of microchannels that are wider and deeper.[37,38,39,40] However, in this study, due to the increasing speed parameter, the laser speed did not form the sharp tip of the microwell structure.

Concave microwells that are deep enough to allow for cell aggregation and spheroid formation are ideal. The laser parameter at 600 mm/s and 20% produced a microwell structure that was suitable for spheroid cultivation; thus, this laser parameter would be applied for the rest of later experiments.

Figure 2C shows the difference in the width of the microwell between the postengraving and the input design. All circle patterns for engraving were designed in the computer with a diameter of 0.4 mm. However, during the investigation of speed and power, the width of microwells was observed to get wider after engraving, compared to the number in the design (>0.4 mm). Since the size of microwells plays a crucial role in determining the size of cancer spheroids, different sizes of circle patterns from 0.1 to 0.6 mm were investigated at 20% and 600 mm/s to select the suitable size of microwells. The results showed a slight increase in microwells' width after engraving. The widest microwell was 0.8 mm, which was engraved from the 0.6 mm circle pattern in the design file. However, the best size for microwells should be 0.4−0.6 mm; thus, in this study, all circle patterns for engraving the microwells were designed as 0.4 mm in the input file before engraving, corresponding to 0.5−0.6 mm after engraving. Figure 2D shows a 3D image of the microwells produced with an engraving parameter speed of 600 mm/s, power of 20%, and design diameter of the microwell of 0.4 mm. The microwells are concave with 0.58 mm width and 0.61 mm depth. One of the important factors in the formation and culture of spheroids was the depth of the concave microwell, as cells in deeper microwells were less susceptible to disturbance by vortexed culture media during washing and refreshing steps. The microwell with a depth of approximately 0.6 mm is suitable for culture cells. Our research results are generally consistent with the trends shown by previous studies.[36,41]

3.2. Synthesis of PEG Microwells. The PMMA mold was fabricated by laser cutting on PMMA sheets with a laser speed of 600 mm/s and 20% power to form microwells after researching the impacts of the laser parameter and validating laser engraving techniques. The complete PMMA mold was inserted into a plastic container and was ready for the fabrication of PDMS molds. The uncured PDMS was viscous; thus, it was able to infiltrate into the microwell structure in PMMA to exactly replicate the structures. After being cured for 48 h at room temperature, PDMS peeled off from the PMMA molds. It was firm and elastic, making it easy to manipulate as a mold for the fabrication of the PEGDA hydrogel platform. To

https://doi.org/10.1021/acsomega.3c05873
ACS Omega 2024, 9, 16949−16958

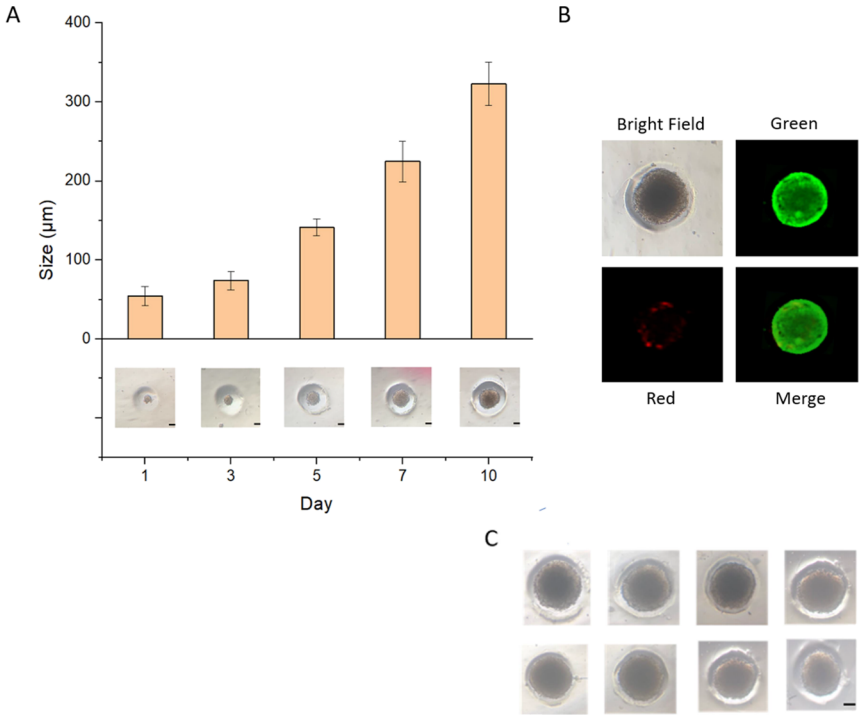

Figure 4. Development of cancer spheroids in microwells. (A) Cancer spheroids growth in 10 days (scale bar = 100 μm). (B) Live/dead assay of cancer spheroids after 10 days of culture with a bright image, green fluorescence (CaAM) for live cells, red fluorescence (EthD-1) for dead cells, and merged images. (C) Homogeneity of the cancer spheres after 10 days (Scale bar = 200 μm) (The experiment was repeated 3 times).

confirm the stability of the laser engraving on the PMMA mold, the average width and depth of 10 microwells on the PMMA die were measured. The results showed high similarity in the width and depth across 10 microwells. The average width and depth of 10 microwells on the PMMA mold were 0.61 ± 0.01 and 0.5 ± 0.02 mm, respectively (Figure 3A).

The accuracy and stability of the laser engraving method for microwell generation were carried out by comparing the width and depth of the microwells on the PMMA, PDMS copying, and PEGDA copying. The results showed a similarity of width and depth in all three types of molds, which indicated PDMS and PEGDA conserved and correctly copied the microwell structure from PMMA molds. The average width of the three molds fluctuated between 0.5 and 0.525 mm, and the depth fluctuated around 0.63 mm (Figure 3B). Additionally, PEG microwells were produced by using PDMS molds that were repeatedly reused. PEG microwells were also molded using a repeatedly reused PDMS template in several other experiments, which demonstrated that the PDMS mold may be used repeatedly without experiencing a major divergence.

The durability of the microwell was surveyed over a period of 21 days. The long-term stability of PEGDA in PBS was followed, and the results show that the microwells do not change over time. In addition, PEGDA physical properties were not significantly altered after processing and were stable to work. These results were also demonstrated in the study of Luong et al.[42]

In this study, the production of PEG microwells was characterized by a short time requirement. The process of using a laser marking machine to create the PMMA mold was done within 1 h. This was followed by a PDMS molding time of 24 h including the mixing, vacuum degassing, and drying process for the PDMS mold. Finally, in order to create PGE microwells, UV light was exposed to the hydrogel mixture for 2 min. In addition, the process was also cost-effective with the cost to create a cell culture plate consisting of 48 microwells including the price of PMMA mold fabrication (0.3 USD), cost of chemicals to create a PDMS mold (0.2 USD) and PEG microwells (0.1 USD). Therefore, the total cost of having a series of microwells was less than 1 USD.

One major feature of this system was the creation of concave PEG microwells. The ideal characteristics of concave microwells promoted the formation of cell aggregates. The cancer cells were seeded onto concave microwells, which impeded cell adhesion resulting in the formation of cancer spheroids as the cells adhered to each other.[43] In addition, the size of the spheroid can be regulated by the cell's concentration and the size of concave microwells.[10,34] Cancer spheroids which are cultured in concave microwells can be used as a more suitable model than the 2D cell monolayer.[43] Therefore, these spheroids are suitable for investigating cell behavior and drug screening. As in the study by Martinov et al. hepatospheres and heterospheres cultured in concave microwells grew in the center of the well and grew uniformly, in contrast to cells cultured on the plane surface or in cylindrical microwells.[31] In addition, Luong's research demonstrated that concave microwell plates are a novel platform for the preparation of an appropriate model for the study of penetration and efficacy of anticancer agents of poorly aggregating cells.[42]

3.3. Formation of 3D Cancer Spheroids. After seeding cancer spheroids into microwells with a concentration of 2 × 10^5 cells/mL, they were cultured for 10 days. On day 1, cells aggregated spontaneously and formed inside the microwell for further growth into 3D spheroids. After 1, 3, 5, 7, and 10 days of culture, the structure of cancer spheroids was confirmed, and Figure 4A depicts the overall size increase of the 3D cells in the structures discovered at a specific time. From day 1 to day 3, the spheroid size slowly increased. After day 5, the cells

https://doi.org/10.1021/acsomega.3c05873
ACS Omega 2024, 9, 16949−16958

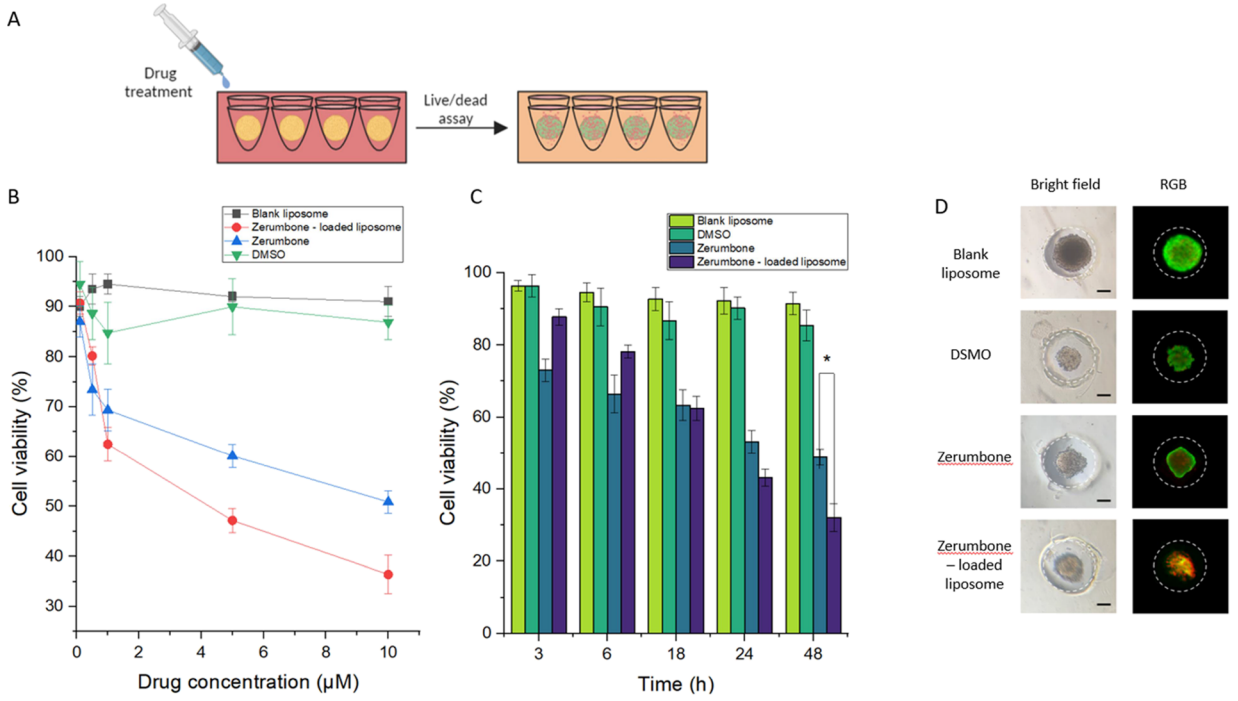

Figure 5. Drug testing on cancer spheroids. (A) Illustration of the effect on cell viability in cancer spheroids during drug treatment. (B) Investigation of the effect of drug concentration on cell viability in cancer spheroids (drug testing period is 24 h). (C) Evaluation of the effect of blank liposomes, zerumbone, and zerumbone-loaded liposomes, DSMO on cancer spheroids over time (concentration of the compounds tested is 5 μM). (*$p > 0.05$) (D) Live/dead essay for spheroids was observed after 48 h treated with blank liposomes, zerumbone, and zerumbone-loaded liposomes, DSMO in bright image, and RGB images. Because zerumbone was solubilized in DMSO, which was toxic to cells, a column on the effects of DMSO on carcinogenic cells was included. The DMSO concentration indicated the quantity of DMSO required to dissolve the zerumbone (scale bar = 150 μm). (The experiment was repeated 3 times).

strongly grew in size. The cells formed on day 1 and day 3 microwells had an average diameter of 50.3 and 55.1 μm, while the spheroid sizes on day 5 and day 7 were 148.4 and 228.6 μm, respectively. The figure for cell size was a significant increase to 320 μm on day 10. These figures were consistent with Chen's study. According to the study by Chen et al. the size of HepG2 spheroids was approximately 42 and 120 μm respectively at day 1 and day 7.[44] In other words, after 6 days, a spheroid grew nearly three times. This demonstrated that HepG2 spheroids formed with a suitable size.

After 10 days of culture, a LIVE/DEAD assay was conducted to test the HepG2 survival rate. Figure 4B shows fluorescent images of HepG2 in which the green indicates the live cells and the red indicates the dead cells. When comparing the ratio between green and red, the percentage of red was approximately 90% while the proportion of green was 10%. This illustrates that the 3D culture method in this study is effective in culturing cancer cells. Figure 4C shows the homogeneity between cancer spheroids after 10 days. The cancer spheroids were observed with a size of 341.4 ± 4.24 μm.

3.4. Drug Testing. Figure 5A illustrates the destruction of cancer cells during drug treatment. The effects of blank liposome, zerumbone, and zerumbone-loaded liposome on the viability of HepG2 cells were evaluated at 24 h after treatment. Figure 5B depicts the effect of different drug concentrations on the cell viability of HepG2. The cell viability remained nearly unchanged as the concentration of blank liposomes dose. When HepG2 was treated with zerumbone and the zerumbone-loaded liposome, cell viability reduced dramatically. Cell viability seemed to decline in a manner similar to that of the low concentration of zerumbone and zerumbone-loaded liposome. Cell death increased more significantly with zerumbone-loaded liposomes than with zerumbone at high concentrations. Cell viability dropped to around 88 and 77% at the two lowest drug doses of 0.1 and 0.5 mg/mL of zerumbone, respectively, while the percentages for liposomes containing zerumbone were 90 and 80%, respectively. Cell viability was significantly reduced after 24 h with zerumbone-loaded liposomes at drug doses of 1 mg/mL. Cell viability at this concentration was 57%. The cell viability of cancer spheroids decreased by 43.2% when the medication concentration was 5 mg/mL. When the medication concentration was 10 mg/mL, the cell viability decreased significantly to 42.3%. The IC_{50} of zerumbone-loaded liposomes is 4.53 pM for 24 h compared with the study of Rahman et al. using zerumbone-loaded nanostructured lipid carrier, the IC_{50} in this study was 5.64 ± 0.38 μg/mL for 72 h.[45] While HepG2 was treated with zerumbone, cell viability decreased to 69, 60, and 51% at drug concentrations of 1, 5, and 10 mg/mL, respectively, after 24 h. This outcome can be elucidated by the continued proliferation of HepG2 cells with great viability, while zerumbone- and zerumbone-loaded liposomes displayed immediate cytotoxic effects on the cells. Furthermore, the results demonstrate that zerumbone-loaded liposomes had the best targeting. The use of zerumbone-loaded liposomes enabled the administration of higher zerumbone concentrations, enhancing the penetration of the compound into HepG2 cells.

HepG2 cells were then tested for viability in 48 h with a 5 mg/mL concentration of blank liposome, zerumbone, and zerumbone-loaded liposome. Figure 5C illustrates the cytotoxic effects of drugs on HepG2 cells over time. The

https://doi.org/10.1021/acsomega.3c05873
ACS Omega 2024, 9, 16949−16958

effect of blank liposomes, zerumbone, and zerumbone-loaded liposomes on HepG2 cells was witnessed at five time points: 3, 6, 18, 24, and 48 h. The HepG2 cell line was not affected by the blank liposomes and it can remain as a positive control, which indicates that blank liposomes allowed cell growth. During the first 6 h, zerumbone was more cytotoxic than zerumbone-loaded liposomes. Regarding to zerumbone, the cell viability rate reduced to 74% during the first 3 h to 67% as the treatment time reached 6 h. While cell viability fell beneath the 85% threshold around 3 h after treatment, a considerable decrease to 78.2% in cell viability of cancer spheroids after 6 h of treatment by zerumbone-loaded liposome. From the 18th hour, zerumbone was less cytotoxic than zerumbone-loaded liposomes. The cytotoxicity activity of zerumbone on HepG2 cells gradually decreased over time, in which the cell viability rate increased to 66%, and 54% after 18 and 24 h, respectively. There was a slow decrease to 48% in HepG2 viability after 48 h by zerumbone. For the zerumbone-loaded liposomes, cell death increased over time more strongly than zerumebone. After 18 and 24 h, the fraction of live cells was almost 63 and 47%, respectively. The cell viability substantially fell by 57.5% when HepG2 was treated with zerumbone-loaded liposome after 48 h. These findings can be explained by the fact that zerumbone had an instantaneous lethal effect on the cells. Liposomes gently release medications, balancing cell growth and death. Furthermore, zerumbone-loaded liposomes can target and release zerumbone in a gradual and regulated manner, damaging more cells. This undoubtedly renders zerumbone-loaded liposomes more successful than free zerumbone in the therapy of illness, particularly cancer.

The in vitro cytotoxicity of zerumbone and zerumbone-loaded nanostructured lipid carriers was examined in the T-cell line in the study by Rahman. The drug released from nanoparticles has numerous benefits over free zerumbone in cancer therapy.[45,46] This is because the only possible difference in the mode of action between zerumbone-loaded nanostructured lipid carriers and zerumbone is that in order to rapid access to zerumbone from zerumbone-loaded nanostructured lipid carriers. For the nanoparticle to target cells, it must initially undergo endocytosis or phagocytosis and then be discharged into the extracellular area. In contrast, unbound zerumbone can directly target cells through passive diffusion.[47] This demonstrates the necessity for a delivery method for zerumbone, such as a zerumbone-loaded liposome, which can address the drug's solubility issue while also acting as a vehicle with improved drug-loading capability.

Abdelwahad et al. studied the role of zerumbone in Caov-3 (ovarian cell lines) and HeLa (cervical cancer cell lines) to Interleukin-6. At 48 h post-treatment, the IL-6 levels for 10, 20, and 30 μM zerumbone-treated HeLa cells reduced by 13.5, 35, and 46% respectively lower compared with the control. While the figures for Caov-3 are 2, 9, 8 and 39%, respectively.[48] These results show that the ability of zerumbone-loaded liposomes to treat cancer in this study is outstanding.

4. CONCLUSIONS

In this study, we successfully generated microwells for cancer spheroid formation by using laser engraving techniques. Results also showed the effects of the laser parameter on the structure of microwells that provided scientific evidence for further studies using laser techniques in fabricating biomedical devices. In addition, the fidelity and stability of the method were verified to form a consistent series of microwells. Besides, PMMA and PDMS molds can be reused to fabricate hydrogel platforms at a lower cost and in less time. PEG microwells also showed stabilization after being stored in PBS for a long time.

The suitable cell seeding concentration inside the microwells was 2×10^5 cells/well was selected for seeding and spheroid formation. The cultivated spheroids grew quickly and with a high percentage of survival in these wells. These spheroids were then treated with zerumbone-loaded liposomes with many concentrations. The results indicated that zerumbone-loaded liposomes had significant liver targeting activity, as compared to zerumbone and it is a suitable ligand for sustainable targeted drug delivery for liver cancer treatments.

■ ASSOCIATED CONTENT

Data Availability Statement

Data sharing is not applicable to this article as no data sets were generated or analyzed during the current study.

■ AUTHOR INFORMATION

Corresponding Authors

Duong Thanh Nguyen − *Institute for Tropical Technology and Graduate University of Science and Technology, Vietnam Academy of Science and Technology (VAST), Hanoi 100000, Vietnam*; Email: ntduong182@gmail.com

Dung Thuy Nguyen Pham − *NTT Institute of Applied Technology and Sustainable Development and Faculty of Environmental and Food Engineering, Nguyen Tat Thanh University, Ho Chi Minh City 70000, Vietnam*; orcid.org/0000-0003-2396-9474; Email: pntdung@ntt.edu.vn

Authors

Mai Anh Nguyen − *Institute for Tropical Technology, Vietnam Academy of Science and Technology (VAST), Hanoi 100000, Vietnam*

Nhung Thi Dinh − *Hanoi University of Science and Technology (HUST), Hanoi 100000, Vietnam*

My Hanh Do Thi − *Institute for Tropical Technology, Vietnam Academy of Science and Technology (VAST), Hanoi 100000, Vietnam*

Dung Nguyen Thi − *Institute for Tropical Technology, Vietnam Academy of Science and Technology (VAST), Hanoi 100000, Vietnam*

Uyen Thu Pham − *Institute for Tropical Technology and University of Science and Technology of Hanoi (USTH), Vietnam Academy of Science and Technology (VAST), Hanoi 100000, Vietnam*

Toan Quoc Tran − *Graduate University of Science and Technology, Vietnam Academy of Science and Technology (VAST), Hanoi 100000, Vietnam; Institute of Natural Products Chemistry, Vietnam Academy of Science and Technology (VAST), Hanoi 100000, Vietnam*

Vuong Minh Nguyen − *Institute of Natural Products Chemistry, Vietnam Academy of Science and Technology (VAST), Hanoi 100000, Vietnam*

Nhung Hong Le − *Graduate University of Science and Technology, Vietnam Academy of Science and Technology (VAST), Hanoi 100000, Vietnam; Institute of Natural Products Chemistry, Vietnam Academy of Science and Technology (VAST), Hanoi 100000, Vietnam*

Complete contact information is available at: https://pubs.acs.org/10.1021/acsomega.3c05873

https://doi.org/10.1021/acsomega.3c05873
ACS Omega 2024, 9, 16949−16958

Author Contributions

Conceptualization: M.A.N., D.T.N., U.T.P., N.T.D. and D.N.T.; methodology: U.T.P.; M.H.D.T. resources: T.Q.T., V.M.N. and T.Q.T.; formal analysis and investigation: U.T.P.; N.H.L., and U.T.P.; data curation: M.A.N., N.T.D., V.M.N. and D.T.N.; validation: M.H.D.T., D.N.T. and U.T.P.; writing—original draft preparation: M.A.N., D.T.N. and U.T.P.; writing—review and editing: D.T.N.P., M.A.N. and N.T.D.; funding acquisition: D.T.N., T.Q.T. and V.M.N.; supervision: M.H.D.T., T.Q.T. and D.T.N.; project administration: V.M.N., T.Q.T. and D.T.N. All authors have read and agreed to the published version of the manuscript.

Funding

This work was supported financially by the Vietnam Ministry of Science and Technology (MOST) for the financial support under project ĐTĐLCN.68/22.

Notes

The authors declare no competing financial interest.

■ ACKNOWLEDGMENTS

We would like to express our gratitude to the Vietnam Ministry of Science and Technology (MOST) for the financial support.

■ REFERENCES

(1) Feng, R.-M.; Zong, Y.-N.; Cao, S.-M.; Xu, R.-H. Current Cancer Situation in China: Good or Bad News from the 2018 Global Cancer Statistics? *Cancer Commun.* **2019**, *39* (1), 1−12.

(2) Sung, H.; Ferlay, J.; Siegel, R. L.; Laversanne, M.; Soerjomataram, I.; Jemal, A.; Bray, F. Global Cancer Statistics 2020: GLOBOCAN Estimates of Incidence and Mortality Worldwide for 36 Cancers in 185 Countries. *CA: A Cancer Journal for Clinicians* **2021**, *71* (3), 209−249.

(3) Zugazagoitia, J.; Guedes, C.; Ponce, S.; Ferrer, I.; Molina-Pinelo, S.; Paz-Ares, L. Current Challenges in Cancer Treatment. *Clinical Therapeutics* **2016**, *38* (7), 1551−1566.

(4) Sudhakar, A. History of Cancer, Ancient and Modern Treatment Methods. *J. Cancer Sci. Ther.* **2009**, *1* (2), 1−4.

(5) Scannell, J. W.; Bosley, J.; Hickman, J. A.; Dawson, G. R.; Truebel, H.; Ferreira, G. S.; Richards, D.; Treherne, J. M. Predictive Validity in Drug Discovery: What It Is, Why It Matters and How to Improve It. *Nat. Rev. Drug Discov* **2022**, *21* (12), 915−931.

(6) Van Norman, G. A. Limitations of Animal Studies for Predicting Toxicity in Clinical Trials: Is It Time to Rethink Our Current Approach? *JACC Basic Transl Sci.* **2019**, *4* (7), 845−854.

(7) Pham, D. T.; Nguyen, L. P.; Pham, Q. T. H.; Pham, C. K.; Pham, D. T. N.; Viet, N. T.; Nguyen, H. V. T.; Tran, T. Q.; Nguyen, D. T. A Low-Cost, Flexible Extruder for Liposomes Synthesis and Application for Murrayafoline A Delivery for Cancer Treatment. *J. Biomater Appl.* **2022**, *37* (5), 872−880.

(8) Bithi, S. S.; Vanapalli, S. A. Microfluidic Cell Isolation Technology for Drug Testing of Single Tumor Cells and Their Clusters. *Sci. Rep* **2017**, *7* (1), 41707.

(9) Ma, L.-D.; Wang, Y.-T.; Wang, J.-R.; Wu, J.-L.; Meng, X.-S.; Hu, P.; Mu, X.; Liang, Q.-L.; Luo, G.-A. Design and Fabrication of a Liver-on-a-Chip Platform for Convenient, Highly Efficient, and Safe in Situ Perfusion Culture of 3D Hepatic Spheroids. *Lab Chip* **2018**, *18* (17), 2547−2562.

(10) Thomsen, A. R.; Aldrian, C.; Bronsert, P.; Thomann, Y.; Nanko, N.; Melin, N.; Rücker, G.; Follo, M.; Grosu, A. L.; Niedermann, G.; Layer, P. G.; Heselich, A.; Lund, P. G. A Deep Conical Agarose Microwell Array for Adhesion Independent Three-Dimensional Cell Culture and Dynamic Volume Measurement. *Lab Chip* **2018**, *18* (1), 179−189.

(11) Lage, O. M.; Ramos, M. C.; Calisto, R.; Almeida, E.; Vasconcelos, V.; Vicente, F. Current Screening Methodologies in Drug Discovery for Selected Human Diseases. *Mar Drugs* **2018**, *16* (8), 279.

(12) Sercombe, L.; Veerati, T.; Moheimani, F.; Wu, S. Y.; Sood, A. K.; Hua, S. Advances and Challenges of Liposome Assisted Drug Delivery. *Front Pharmacol* **2015**, *6*, 286.

(13) Edmondson, R.; Broglie, J. J.; Adcock, A. F.; Yang, L. Three-Dimensional Cell Culture Systems and Their Applications in Drug Discovery and Cell-Based Biosensors. *Assay Drug Dev Technol.* **2014**, *12* (4), 207−218.

(14) Do, T. D.; Pham, U. T.; Nguyen, L. P.; Nguyen, T. M.; Bui, C. N.; Oliver, S.; Pham, P.; Tran, T. Q.; Hoang, B. T.; Pham, M. T. H.; Pham, D. T. N.; Nguyen, D. T. Fabrication of a Low-Cost Microfluidic Device for High-Throughput Drug Testing on Static and Dynamic Cancer Spheroid Culture Models. *Diagnostics* **2023**, *13* (8), 1394.

(15) Zhang, C.; Yang, Z.; Dong, D.-L.; Jang, T.-S.; Knowles, J. C.; Kim, H.-W.; Jin, G.-Z.; Xuan, Y. 3D Culture Technologies of Cancer Stem Cells: Promising Ex Vivo Tumor Models. *J. Tissue Eng.* **2020**, *11*, No. 2041731420933407.

(16) De Pieri, A.; Rochev, Y.; Zeugolis, D. I. Scaffold-Free Cell-Based Tissue Engineering Therapies: Advances, Shortfalls and Forecast. *npj Regen Med.* **2021**, *6* (1), 1−15.

(17) Topouzi, H.; Logan, N. J.; Williams, G.; Higgins, C. A. Methods for the Isolation and 3D Culture of Dermal Papilla Cells from Human Hair Follicles. *Experimental Dermatology* **2017**, *26* (6), 491−496.

(18) Mehta, G.; Hsiao, A. Y.; Ingram, M.; Luker, G. D.; Takayama, S. Opportunities and Challenges for Use of Tumor Spheroids as Models to Test Drug Delivery and Efficacy. *J. Controlled Release* **2012**, *164* (2), 192−204.

(19) Yip, D.; Cho, C. H. A Multicellular 3D Heterospheroid Model of Liver Tumor and Stromal Cells in Collagen Gel for Anti-Cancer Drug Testing. *Biochem. Biophys. Res. Commun.* **2013**, *433* (3), 327−332.

(20) Kwapiszewska, K.; Michalczuk, A.; Rybka, M.; Kwapiszewski, R.; Brzózka, Z. A Microfluidic-Based Platform for Tumour Spheroid Culture, Monitoring and Drug Screening. *Lab Chip* **2014**, *14* (12), 2096−2104.

(21) Zhang, W.; Zhuang, A.; Gu, P.; Zhou, H.; Fan, X. A Review of the Three-Dimensional Cell Culture Technique: Approaches, Advantages and Applications. *Current Stem Cell Research & Therapy* **2016**, *11* (4), 370−380.

(22) Du, G.; Fang, Q.; den Toonder, J. M. J. Microfluidics for Cell-Based High Throughput Screening Platforms—A Review. *Anal. Chim. Acta* **2016**, *903*, 36−50.

(23) Fernandes, T. G.; Diogo, M. M.; Clark, D. S.; Dordick, J. S.; Cabral, J. M. S. High-Throughput Cellular Microarray Platforms: Applications in Drug Discovery, Toxicology and Stem Cell Research. *Trends Biotechnol.* **2009**, *27* (6), 342−349.

(24) Feng, G.-H.; Tsai, M.-Y. Acoustic Emission Sensor with Structure-Enhanced Sensing Mechanism Based on Micro-Embossed Piezoelectric Polymer. *Sensors and Actuators A: Physical* **2010**, *162* (1), 100−106.

(25) Broers, A. N.; Hoole, A. C. F.; Ryan, J. M. Electron Beam Lithography—Resolution Limits. *Microelectron. Eng.* **1996**, *32* (1), 131−142.

(26) Thomas, M. S.; Millare, B.; Clift, J. M.; Bao, D.; Hong, C.; Vullev, V. I. Print-and-Peel Fabrication for Microfluidics: What's in It for Biomedical Applications? *Ann. Biomed Eng.* **2010**, *38* (1), 21−32.

(27) Vasylieva, N.; Marinesco, S.; Barbier, D.; Sabac, A. Silicon/SU8Multi-Electrode Micro-Needle for in Vivo Neurochemical Monitoring. *Biosens. Bioelectron.* **2015**, *72*, 148−155.

(28) Liu, J.; Song, D.; Zong, G.; Yin, P.; Zhang, X.; Xu, Z.; Du, L.; Liu, C.; Wang, L. Fabrication of SU-8 Moulds on Glass Substrates by Using a Common Thin Negative Photoresist as an Adhesive Layer. *J. Micromech. Microeng.* **2014**, *24* (3), No. 035009.

(29) Sun, T.; Kovac, J.; Voldman, J. Image-Based Single-Cell Sorting via Dual-Photopolymerized Microwell Arrays. *Anal. Chem.* **2014**, *86* (2), 977−981.

https://doi.org/10.1021/acsomega.3c05873
ACS Omega 2024, 9, 16949−16958

(30) Matsui, S. Three-Dimensional Nanostructure Fabrication by Focused Ion Beam Chemical Vapor Deposition. In *Springer Handbook of Nanotechnology*; Bhushan, B., Ed.; Springer Handbooks; Springer: Berlin, Heidelberg, 2007; pp. 179−196.
(31) Martinov, G. M.; Obuhov, A. I.; Martinova, L. I.; Grigoriev, A. S. An Approach to Building a Specialized CNC System for Laser Engraving Machining. *Procedia CIRP* **2016**, *41*, 998−1003.
(32) Kumar, P.; Tarun, A.; Gowtham, M.; Thamma, P.; Yashwanth, G. Design and Fabrication of Portable Laser Cutting and Engraving Machine. *Int. J. Eng. Technol.* **2017**, *7*, 570.
(33) Chen, Y.-W.; Chen, M.-C.; Wu, K.-W.; Tu, T.-Y. A Facile Approach for Rapid Prototyping of Microneedle Molds, Microwells and Micro-Through-Holes in Various Substrate Materials Using CO2 Laser Drilling. *Biomedicines* **2020**, *8* (10), 427.
(34) Guo, W.; Chen, Z.; Feng, Z.; Li, H.; Zhang, M.; Zhang, H.; Cui, X. Fabrication of Concave Microwells and Their Applications in Micro-Tissue Engineering: A Review. *Micromachines (Basel)* **2022**, *13* (9), 1555.
(35) Tu, T.-Y.; Wang, Z.; Bai, J.; Sun, W.; Peng, W. K.; Huang, R. Y.-J.; Thiery, J.-P.; Kamm, R. D. Rapid Prototyping of Concave Microwells for the Formation of 3D Multicellular Cancer Aggregates for Drug Screening. *Adv. Healthc Mater.* **2014**, *3* (4), 609−616.
(36) Wu, K.; Kuo, C.; Tu, T. A Highly Reproducible Micro U-Well Array Plate Facilitating High-Throughput Tumor Spheroid Culture and Drug Assessment. *Glob Chall* **2021**, *5* (2), No. 2000056.
(37) Dinh, C. T.; Vu, H. T.; Phan, Q. T. H.; Nguyen, L. P.; Tran, T. Q.; Van Tran, D.; Quy, N. N.; Pham, D. T. N.; Nguyen, D. T. Synthesis of Glycyrrhetinic Acid-Modified Liposomes to Deliver Murrayafoline A for Treatment of Hepatocellular Carcinoma. *J. Mater. Sci: Mater. Med.* **2022**, *33* (10), 72.
(38) Khanafi-Benghalem, N.; Benghalem, K.; Boudoukha, H. Effect Of Laser CO2 Parameters In Marking Of Glass. *AIP Conf. Proc.* **2008**, *1047* (1), 204−207.
(39) Sun, Y.; Kwok, Y. C.; Nguyen, N.-T. Low-Pressure, High-Temperature Thermal Bonding of Polymeric Microfluidic Devices and Their Applications for Electrophoretic Separation. *J. Micromech. Microeng.* **2006**, *16* (8), 1681.
(40) Gabriel, E. F. M.; Coltro, W. K. T.; Garcia, C. D. Fast and Versatile Fabrication of PMMA Microchip Electrophoretic Devices by Laser Engraving. *ELECTROPHORESIS* **2014**, *35* (16), 2325−2332.
(41) Khoo, B. L.; Grenci, G.; Lim, Y. B.; Lee, S. C.; Han, J.; Lim, C. T. Expansion of Patient-Derived Circulating Tumor Cells from Liquid Biopsies Using a CTC Microfluidic Culture Device. *Nat. Protoc* **2018**, *13* (1), 34−58.
(42) Luong, P. T.; Browning, M. B.; Bixler, R. S.; Cosgriff-Hernandez, E. Drying and Storage Effects on Poly(Ethylene Glycol) Hydrogel Mechanical Properties and Bioactivity. *J. Biomed. Mater. Res., Part A* **2014**, *102* (9), 3066−3076.
(43) Cha, J. M.; Park, H.; Shin, E. K.; Sung, J. H.; Kim, O.; Jung, W.; Bang, O. Y.; Kim, J. A Novel Cylindrical Microwell Featuring Inverted-Pyramidal Opening for Efficient Cell Spheroid Formation without Cell Loss. *Biofabrication* **2017**, *9* (3), No. 035006.
(44) Chen, K.; Wu, M.; Guo, F.; Li, P.; Chan, C. Y.; Mao, Z.; Li, S.; Ren, L.; Zhang, R.; Huang, T. J. Rapid Formation of Size-Controllable Multicellular Spheroids via 3D Acoustic Tweezers. *Lab Chip* **2016**, *16* (14), 2636−2643.
(45) Rahman, H. S.; Rasedee, A.; How, C. W.; Abdul, A. B.; Zeenathul, N. A.; Othman, H. H.; Saeed, M. I.; Yeap, S. K. Zerumbone-Loaded Nanostructured Lipid Carriers: Preparation, Characterization, and Antileukemic Effect. *Int. J. Nanomed.* **2013**, *8* (1), 2769−2781, DOI: 10.2147/IJN.S45313.
(46) Rahman, H. S.; Rasedee, A.; Abdul, A. B.; Zeenathul, N. A.; Othman, H. H.; Yeap, S. K.; How, C. W.; Hafiza, W. A. G. W. N. Zerumbone-Loaded Nanostructured Lipid Carrier Induces G2/M Cell Cycle Arrest and Apoptosis via Mitochondrial Pathway in a Human Lymphoblastic Leukemia Cell Line. *Int. J. Nanomed.* **2014**, *9*, 527−538.
(47) Chen, C.-H.; Miller, M. A.; Sarkar, A.; Beste, M. T.; Isaacson, K. B.; Lauffenburger, D. A.; Griffith, L. G.; Han, J. Multiplexed Protease Activity Assay for Low-Volume Clinical Samples Using Droplet-Based Microfluidics and Its Application to Endometriosis. *J. Am. Chem. Soc.* **2013**, *135* (5), 1645−1648.
(48) Abdelwahab, S. I.; Abdul, A. B.; Zain, Z. N. M.; Hadi, A. H. A. Zerumbone Inhibits Interleukin-6 and Induces Apoptosis and Cell Cycle Arrest in Ovarian and Cervical Cancer Cells. *International Immunopharmacology* **2012**, *12* (4), 594−602.

https://doi.org/10.1021/acsomega.3c05873
ACS Omega 2024, 9, 16949−16958